100 YEARS Journal of Ecology

British Ecological Society

Journal of Ecology 2016, **104**, 315–330 doi: 10.1111/1365-2745.12545

DEMOGRAPHY BEYOND THE POPULATION

Forest community response to invasive pathogens: the case of ash dieback in a British woodland

Jessica Needham[1]*, Cory Merow[2], Nathalie Butt[3], Yadvinder Malhi[4], Toby R. Marthews[4], Michael Morecroft[5] and Sean M. McMahon[6]

[1]Department of Plant Sciences, University of Oxford, Oxford, OX1 3RB, UK; [2]Ecology and Evolutionary Biology, University of Connecticut, 75 N. Eagleville Road, Unit 3043, Storrs, CT 06268, USA; [3]School of Biological Sciences, ARC Centre of Excellence for Environmental Decisions, The University of Queensland, St Lucia, QLD 4072, Australia; [4]School of Geography and the Environment, Environmental Change Institute, University of Oxford, South Parks Road, Oxford OX1 3QY, UK; [5]Natural England, Cromwell House, 15 Andover Road, Winchester SO23 7BT, UK; and [6]Smithsonian Institution Forest Global Earth Observatory, Smithsonian Environmental Research Center, 647 Contees Wharf Road, Edgewater, MD 21307-0028, USA

Summary

1. Large-scale mortality events in forests are increasing in frequency and intensity and can lead to both intermediate- and long-term changes in these systems. Specialist pests and pathogens are unique disturbances, as they commonly target individual species that are relatively prevalent in the community.

2. Understanding the consequences of pathogen-caused mortality requires using sometimes limited available data to create statistical models that can forecast future community states.

3. In the last two decades, ash dieback disease has swept through Europe causing widespread mortality of *Fraxinus excelsior* L. (European ash) across much of its distribution. In the UK, *F. excelsior* is an abundant and ecologically important species.

4. Using demographic data from an 18 ha plot in Wytham Woods, Oxfordshire, we built models that forecast the response of this forest plot to the loss of *F. excelsior*. We combine integral projection models and individual-based models to link models of growth, survival and fecundity to population dynamics. We demonstrate likely responses in Wytham by comparing projections under different levels of *F. excelsior* mortality. To extrapolate results to other systems, we test hypotheses regarding the role of abundance, spatial structure and demographic differences between species in determining community response to disease disturbance.

5. We show that the outcome of succession is determined largely by the differing demographic strategies and starting abundances of competing species. Spatial associations between species were shown to have little effect on community dynamics at the spatial scale of this plot.

6. *Synthesis*. Host-specific pests and pathogens are an increasingly important type of disturbance. We have developed a framework that makes use of forest inventory data to forecast changes in the population dynamics of remaining species and the consequences for community structure. We use our framework to predict how a typical British woodland will respond to ash dieback disease and show how vital rates, spatial structure and abundance impact the community response to the loss of a key species.

Key-words: Bayesian inference, disease disturbance, forest demography, individual-based models, integral projection models, inverse models, plant population and community dynamics

Introduction

Global change driven by anthropogenic activities has resulted in a rising threat to forests from both native and introduced pests and pathogens (Brasier 2008). Pests and pathogens that cause high mortality rates in the host species can have a

*Correspondence author. E-mail: jessica.needham@plants.ox.ac.uk

This article forms part of the British Ecological Society journals' Demography Beyond the Population special feature http://wileyonlinelibrary.com/BES_demography

profound impact on forest structure and function (Logan & Powell 2001). The most recent Forest Resources Assessment indicates that close to 40 million hectares of forested land were adversely affected by disease or insect outbreaks in 2005 (FAO, 2010).

Not surprisingly, the negative impact of forest pathogens is predicted to be greatest when the target is a dominant species (Ellison *et al.* 2005; Loo 2009). The ecosystem effects of epidemics in dominant tree species are well documented and include changes to ecosystem processes (Hicke *et al.* 2012) and declines in populations of dependent species (Tingley *et al.* 2002). Further, the loss of a dominant species can have a cascading impact on the forest as large mortality events can lead to other disturbances, such as increased fire risk, or the facilitation of an aggressive, non-native species. The loss of a dominant species from an ecosystem provides the opportunity to study the role of a single species in structuring community dynamics and regulating ecosystem processes, as well as determining the successional changes that take place upon its removal.

The decline in eastern hemlock, *Tsuga canadensis*, from North America due to the hemlock woolly adelgid, *Adelges tsugae*, has led to substantial changes in the microenvironment of the forest understorey and a dramatic increase in the abundance of invasive plant species (Eschtruth *et al.* 2006; Ford *et al.* 2012). Another example is the mountain pine beetle *Dendroctonus ponderosae*, which has caused widespread mortality in *Pinus contorta* and *Pinus ponderosa* forests throughout the Rocky Mountains from Mexico to Canada. The reduction in carbon uptake and the increase in wood decomposition are great enough to have converted the affected region from a net carbon sink to a carbon source (Kurz *et al.* 2008). The focus of this study, *Fraxinus excelsior* (European ash), is a dominant species in many woodlands across Britain (National Forest Inventory 2012) and its expected decline due to the pathogen *Hymenoscyphus fraxineus* is likely to have important consequences for forest composition and biodiversity (Mitchell *et al.* 2014).

ASH DIEBACK

Ash dieback disease is a current epidemic in Europe, caused by the fungal pathogen *H. fraxineus* (Gross *et al.* 2014). Significant numbers of diseased *F. excelsior* were first recorded in Poland in the early 1990s (Przybyl 2002) and since then the fungus has spread rapidly causing widespread mortality of *F. excelsior* across its entire European distribution (McKinney *et al.* 2014). The pathogen targets all size classes, although symptoms and eventual mortality progress more rapidly in smaller individuals (Keßler *et al.* 2012). Progeny trials in Scandanavia predict that just 1% of natural populations will have resistance (Kjær *et al.* 2012). However, while infection rates are high across Europe, there is substantial variation in mortality rates (Vasaitis & Lygis 2008; Pliūra *et al.* 2011; Kirisits & Freinschlag 2012; McKinney *et al.* 2014).

FORECASTING FOREST DYNAMICS

How can we predict community responses in the aftermath of a dramatic disturbance? Classic theory on succession predicts that pioneer species will benefit from the disturbance caused by the loss of a dominant species, for example due to pest and pathogens or selective harvesting (Whitmore 1998). However, spatial structure and pre-disturbance abundances are also important (Frelich & Reich 1995). The spatial and temporal patterns of mortality influence the size and frequency of gap formation, with different gap sizes being associated with recruitment by different species (Kneeshaw & Bergeron 1998). In addition, the initial abundance of each species can influence community trajectories following disturbance. Abundant species may have an initial recruitment advantage because they produce more seeds or are closer, on average, to gaps. But in the presence of superior competitors with faster growth rates or higher survival and fecundity, this advantage may be quickly lost and even abundant species can decline in relative dominance (Clebsch & Busing 1989).

Fraxinus excelsior is ecologically important in a variety of forest and non-forest settings. Nevertheless, the consequences of ash dieback disease on forest ecosystems have not been well documented (but see Jönsson & Thor 2012; McKinney *et al.* 2012). Throughout Europe, *F. excelsior* plays a keystone role in riparian forest ecosystems (Pautasso *et al.* 2013). It is especially abundant in Britain, making up 14% of broadleaved forest standing volume nationally (National Forest Inventory 2012), and is often dominant at smaller spatial scales. In many countries, *F. excelsior* was clear-felled either upon infection by *H. fraxineus* or pre-emptively. Studies from clear-felled natural forest sites suggest very little *F. excelsior* regeneration and a shift towards increased abundance of other species (Lygis *et al.* 2014). However, we predict that succession will play out differently where the epidemic is left to run its course, as the time scale over which mortality occurs among different size classes differentially impacts regeneration across species.

Here, we develop a predictive framework to test hypotheses about responses to the anticipated loss of *F. excelsior* due to ash dieback disease. We combine population- and community-level models to forecast succession in our study plot and similar woodlands and address the following hypotheses:

H1: The severity of *F. excelsior* mortality will determine the post-disturbance dynamics. Specifically, we expect the *F. excelsior* population to show limited or no recovery once the population is reduced beyond a certain threshold. As a result, we expect remaining tree species to show short-term regeneration when *F. excelsior* mortality is low, and more sustained increases in basal area (BA) and population size when *F. excelsior* mortality is high.

H2: Increases in population size and BA of remaining species will depend on demographic rates, as oppose to initial abundances. Thus, *Acer pseudoplatanus* will be capable of significant increases even when it starts with a small population size.

H3: Spatial associations between *F. excelsior* and other species will determine patterns of regeneration.
H4: Under all mortality scenarios, the total BA and the total number of trees of all species will recover to pre-disturbance levels within 100 years, although the size structure will shift as the gaps left by the mortality of large *F. excelsior* trees get filled by smaller recruits.

We conclude by generalizing our insights to other forest ecosystems faced with disturbance from pests or pathogens.

Materials and methods

SITE DESCRIPTION

Our study area is the 18 ha permanent plot in Wytham Woods, Oxfordshire, UK (51.77 N, −1.34 W). For details on Wytham Woods and its management history, see Morecroft *et al.* (2008) and Savill *et al.* (2010). Wytham Woods is typical of southern England, with a temperate climate that rarely experiences either snow or temperatures above 30 °C (Butt *et al.* 2009). The plot lies in an area of disturbed, ancient, semi-natural woodland with a small section of secondary woodland and an abandoned small-scale plantation.

Data from 164 100 m^2 monitoring plots across Wytham showed that since 1974, the occurrence and BA of *A. pseudoplatanus* and other canopy species such as *Quercus robur* and *Fagus sylvatica* has been relatively stable while *F. excelsior* has increased in both frequency and BA (Kirby *et al.* 2014). As is typical in other woodlands (Waters & Savill 1992), *F. excelsior* has also dominated regeneration in Wytham in the last few decades (accounting for 75% of seedlings in 2012), while *Q. robur* and *F. sylvatica* show virtually no regeneration (Kirby *et al.* 2014). High mortality of *F. excelsior* could, therefore, leave significant canopy gaps and an opening of the understorey. The fungal pathogen, *H. fraxineus,* has been observed in nearby woodlands, but not yet in Wytham Woods (http://chalaramap.fera.defra.gov.uk/). We expect it to arrive in the next few years.

DATA

The forest plot is part of the Smithsonian Institution's Forest Global Earth Observatory network of plots (http://www.forestgeo.si.edu/), and data collection follows a standardized protocol (Condit 1998). The 18 ha plot is arranged as a 6 × 3 ha grid, with each hectare further divided into 25 20 × 20 m subplots. In the plot, all woody stems greater than 1 cm diameter at breast height (d.b.h.) are measured, identified and mapped. Measurements of d.b.h. were at a marked point of measure. This census was conducted twice, in 2008 and 2010. In total, more than 20 300 stems of 24 different species were recorded over the two censuses (Butt *et al.* 2009). The plot lies in an area of relatively young growth (<150 years) with few very large trees relative to the large number of smaller stems (See Fig. S1 in Supporting Information).

We used observations of 16 188 individuals from censuses 2 years apart. This census interval is relatively short compared with the life span of a canopy tree. The census years were representative of the climate over the 30 preceding years (Fig. S2) with the exception of November 2009, which had 86 mm more precipitation than average, and December 2010 which was 3.3 °C colder than average (CRU CL2.0). Building models from such a short census interval represents a critical challenge in managing forests under global change. Even censuses 1–2 decades apart represent a short window in the life span of most trees, and with many forests world-wide uncensussed, the prospect of obtaining data over longer intervals is extremely limited.

SPECIES GROUPINGS

The four most abundant species were treated separately, and the remaining species were pooled into either sub-canopy or canopy groupings according to life-form (Table S1). The four most abundant species, which together made up 94% of stems, were *A. pseudoplatanus* (sycamore), *F. excelsior* (European ash), both canopy species, *Crataegus monogyna* (hawthorn) and *Corylus avellana* (hazel), both sub-canopy species. Remaining species had too few individuals across the size distribution to infer vital rates parameters at the species level. Pooled rare species are referred to as 'rare sub-canopy' and 'rare canopy'.

MODELS AND SIMULATIONS

Simulation overview

The workflow proceeds in three stages. In the 'Vital Rate Models', we first develop novel functions to describe individual vital rates and use Bayesian MCMC methods (Hastings 1970; Gelman & Hill 2007; Gelman *et al.* 2013) to estimate species-specific parameters directly from the census data. In 'Inverse Estimation from Integral Projection Models (IPMs)', we take an inverse modelling approach to estimate vital rate parameters that could not be inferred from the census data (fecundity and several survival parameters). For each species or pooled species group, this involves a second Bayesian MCMC analysis in which we use population-level summary statistics from IPMs to estimate 'missing' individual-level vital rates parameters. Finally, in 'Forward projection with an individual-based model (IBM)', we use vital rates parameters derived from the IPM analysis to drive spatially explicit IBMs that test how different mechanisms – spatial structure, ash dieback severity and interspecific demographic variation – differentially influence forest dynamics within our study plot (Fig. 1).

Vital rates models

Survival: a mixture of logistic functions. Survival between censuses was recorded as a binary variable. For each species, survival probability was modelled as a function of individual size x using two five-parameter logistic functions that meet at a species-specific size threshold k (eqn 1). This approach is similar to a generalized additive model and captures the high mortality of small trees, followed by the increase and plateau in survival before a gradual senescence at larger sizes. The five-parameter form offers a flexible way of adjusting the lower and upper asymptotes of survival probability along with the rate and symmetry of change and the size at which it occurs (Fig. S3). By splicing together two logistic functions, we ensure that the many observations at small sizes do not influence parameter estimates at sizes that have fewer data due to the numerical dominance of small individuals. The survival function takes the form:

$$\mathrm{logit}(s) = \left(L1 + \frac{K1 - L1}{\left(1 + \left(1/\theta 1 e^{-r1_{\theta 1}^{x-p1}}\right)\right)^{\theta 1}} \right)^{t} \quad x < k, \qquad \text{eqn 1}$$

$$\mathrm{logit}(s) = \left(L2 + \frac{K2 - L2}{\left(1 + \left(1/\theta 2 e^{-r2_{\theta 2}^{x-p2}}\right)\right)^{\theta 2}} \right)^{t} \quad x \geq k, \qquad \text{eqn 2}$$

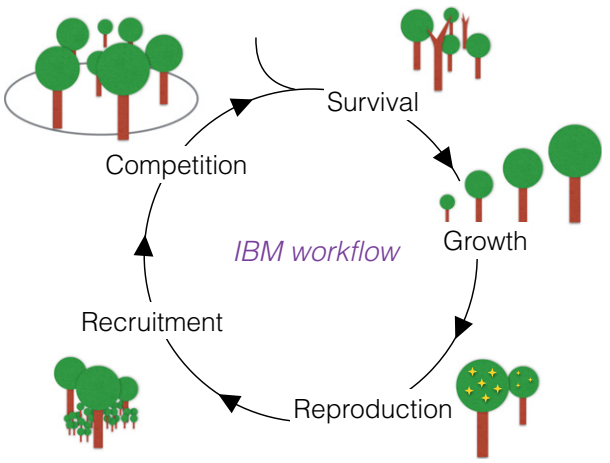

Fig. 1. Schematic of the individual-based model. Each year trees survive or die as a function of their diameter at breast height (d.b.h.). Surviving trees grow with an increment drawn from a distribution dependent on their species and light environment. Individuals with d.b.h. above a reproductive threshold produce offspring. During the recruitment stage offspring are distributed between subplots based on the basal area (BA) of reproductive adults. Density dependence thins the new recruits, removing recruits from areas with a high density of recruits and a high BA of all trees. Competition is recalculated each year and determines the light environment of each individual. The individual-based model is parameterised from a mix of vital rates models fit to census data, and inverse models which infer parameter values for which there were no data.

where L and K are the lower and upper asymptotes of the survival curve, respectively; θ, r and p are the symmetry, rate and inflection point of the curve, respectively; x is d.b.h.; t is time in years between census intervals; and k is the size threshold at which the curves meet. For small individuals, $r1$ is constrained positive, such that survival probability increases with increasing size. For large adults, $r2$ is constrained negative so that survival probability decreases with increasing size. $K1$ is always equal to $K2$ to ensure the two curves meet without sharp changes in survival probability with size. The parameters for each curve, and the size threshold at which the curves meet, were all inferred using Bayesian MCMC analysis (Fig. S4 and Table S3).

Growth: distributional models with flexible variance structure. Growth increment was based on absolute change in d.b.h.. We assumed that the apparent dramatic shrinkage (>6 mm) or growth (>50 mm) of a number of trees was due to measurement error, and these trees (29) were removed from further analysis. We corrected for smaller measurement errors following the method described by Rüger & Condit (2012).

We assumed that growth was determined by the light environment of each individual. The growth increment data collected at Wytham was highly right-skewed with the majority of individuals growing very little each year and a small minority having much larger increments (Fig. S5). We, therefore, fit two distributions to the growth data for each species; a log-normal distribution describing the low mean and right skew of the majority of growth increments, $z \sim \text{lognorm}(\mu, \sigma)$ and a truncated normal describing the higher mean and more symmetric distribution of the fastest growers, $z \sim \text{truncnorm}(\mu, \sigma, \alpha, b)$, where z is increment in mm, μ and σ are the species-specific mean and standard deviation of each distribution, and α and b are 0 and ∞, respectively, to prevent negative growth.

We assumed that the slow-growing individuals were those experiencing low-light conditions, and the fast-growing individuals were those experiencing high-light conditions; either in gaps or because they were tall enough to reach the canopy. Indirectly inferring light environment in this way is a critical step for capturing crucial individual-level variation that drives forest dynamics by taking advantage of typical census data where environmental covariates are unavailable.

For each species, we fit the log-normal distribution to the slowest 95% of increment data and the truncated normal to the fastest 5% of increment data. This reflects the general probability that non-canopy individuals have access to high light during the year. For the three species with the potential to reach canopy height (*A. pseudoplatanus*, *F. excelsior* and 'rare canopy'), we also defined a size threshold of 250 mm d.b.h., where growth from individuals above this size also contributed to the 'fast' growth distribution. This step is based on the assumption that individuals with a d.b.h. above 250 mm are tall enough to have reached the canopy and are, therefore, in high light and not subject to the constraints of low-light environments. These individuals do, however, contribute a few small increments to the fast growth distribution. Species-specific parameters were inferred using Bayesian MCMC methods (Fig. S6 and Table S4).

Inverse estimation from IPMs

Key limitations in available data create challenges to predicting whole forest dynamics, especially for projection where all life history stages need to be included in the model. Common monitoring protocols often lack data on seed production and germination and seedling transitions due to logistical constraints (Comita *et al.* 2007). Further, once trees escape high seedling and sapling mortality, they generally have high survival throughout their lifetimes (>97% survival per annum). Mortality events are rare and highly stochastic, meaning that few deaths of larger individuals or rare species are recorded in a typical short census interval. These challenges led us to the use of inverse models.

Inverse models use simulation output to describe parameters that have no *a priori* likelihood (Hartig *et al.* 2014). We fit inverse models to infer demographic transitions without direct observation of those transitions (Wood 1997). For example, population size is the outcome of survival, growth and reproduction, and it can be used to infer parameter values for each of these vital rates in stage structured models (González & Martorell 2013) or in unstructured models (Besbeas, Lebreton & Morgan 2003). Using the survival and growth parameters inferred above, which is derived from extensive data, along with initial estimates of fecundity parameters, we inferred a fecundity value for all species groups that would (i) reflect approximate long-term recruitment, so that the species had the potential to contribute to forest structure and (ii) demonstrate low overall sensitivity of dynamics to this estimated recruitment component. To do this, we constructed IPMs (Easterling, Ellner & Dixon 2000; Merow *et al.* 2014) to project populations with continuous stage structure (e.g. individual size) forward in time based on a transition 'kernel' that describes the size dependence of survival, growth and offspring production [analogous to matrix population models described by Caswell (2001) and Morris & Doak (2002)], and we used the output of these IPMs to determine population growth rate, λ. This enables us to run an inverse estimation of recruitment that maintained a general population stability across the forest community. The proposed 'missing' parameters are accepted or rejected in a Bayesian MCMC analysis based on the fit of the eigenvalues from the IPMs to $\lambda = 1$. In this

way, population summary statistics (λ) feedback to inform individual-level parameters which could not be estimated directly from the census data (fecundity, and $p1$, $p2$, $r1$ and $r2$) (see Hartig *et al.* 2014; Beaumont 2010 for a more comprehensive description of inverse models and approximate Bayesian computation methods).

As in Cobb *et al.* (2012), in our inverse models, we make the assumption that the population is stable (population growth rate, λ, equal to one) to infer fecundity and missing survival parameters. There are two apparent drawbacks to this approach. Firstly, there are multiple combinations of parameters that can give rise to a megamatrix with $\lambda = 1$. However, since the growth parameters and the majority of survival parameters are fixed, we are only finding a limited number of parameters that, in combination with these fixed parameters, give a $\lambda = 1$, and this greatly reduces the parameter space that needs to be searched and the possible values that can be inferred.

Secondly, the assumption of $\lambda = 1$ itself could be seen as problematic given that the populations in Wytham are surely not at equilibrium. However, it is important to note that these parameters are for IPMs which model each species in isolation. These IPMs are a tool to enable us to parameterize a spatially explicit IBM in which interactions between species, including competition and density dependence, combine with spatially dependent processes such as seed dispersal, in order to determine community dynamics. A species with parameters giving it a $\lambda = 1$ in the IPM is unlikely to be stable in the IBM when these other processes operate. Crucially, it enables us to infer fecundity and survival parameters which could not be directly estimated without decades of further data collection.

Fecundity. To construct IPMs that model the full life history of a population, we need a fecundity function describing the production of offspring and the distribution of offspring sizes. We made three assumptions about the probability of reproduction by each individual: (i) there is a reproductive size threshold below which individuals cannot reproduce, (ii) the probability of producing offspring scales with BA and (iii) the probability of reproduction by trees is different in low- and high-light environments (eqn 3).

The number of recruits, r, produced per individual of d.b.h. x is given by:

$$r = \pi\left(\frac{x}{2}\right)^2 \times f_{ij} \quad \text{for all } x \geq D_i, \qquad \text{eqn 3}$$

where f_{ij} is the fecundity parameter corresponding to the species i in light environment j (j = high or low), and D_i is the reproductive size threshold for species i.

We estimated D as the 0.8th quantile of d.b.h. measurements for each species, with the exception of 'rare canopy' species where we capped D at 250 mm (due to an ageing population of *Q. robur* the 0.8th d.b.h. quantile of 'rare canopy' species was 620 mm – much larger than known reproductive size). Further, for the three species where individuals have the potential to reach the canopy, we assumed that only those individuals in the fast growth distribution corresponding to high light would be reproductive (Fig. S7 and Table S5). We model the distribution of offspring sizes as 10 mm plus 1 year's increment from the slow growth distribution.

IPMs with multiple light environments

To construct IPMs that move individuals between light environments characterized by high and low growth and fecundity functions, we follow the method of Caswell (2012), adapting an age by stage modelling framework to environment by stage and replacing standard population matrices with IPM matrices. This results in so-called megamatrices, in which each element of a megamatrix describes the product of the transitions between environmental conditions and the integral projection kernel describing the full life history of the species (Fig. S8).

In our models, the megamatrix described transitions between low- and high-light environments, similar to those used by Metcalf *et al.* (2009), who modelled the trajectories of individuals based on continuous growth determined by transitions between nine different light environments. However, whereas Metcalf *et al.* (2009) had direct observations of the transitions between light environments, these are lacking for Wytham. We, therefore, calculated transition probabilities from the overlap of each growth distribution with the increment threshold that is used to delimit the two distributions (corresponding to the 0.95th quantile of increment data) (Fig. S9). In other words, the proportion of the log-normal distribution (describing slow growth in low light) that is above the increment corresponding to the 0.95th quantile of all increment data was used as the transition probability from low light to high light. Likewise, the proportion of the truncated normal (describing fast growth in high light) that was below the 0.95thth quantile of all increment data, described the transition probability from high light to low light. The distribution of offspring into high- and low-light environments matched the transition probabilities between light environments by adult trees of that species, regardless of parent size or light environment.

Forward projection with an IBM

To combine the dynamics of multiple species, we used parameters from the IPMs in spatially explicit IBMs. Our IPMs ignore individual differences, except as far as they are captured by the individual size and light environment state variables. However, spatial structure can be a key to determining community dynamics and can only be described at the individual level. Hence, we adopted an IBM framework that allowed us to use the vital rate models fitted with the inverse model to simulate forest dynamics while reflecting individual-level spatial structure.

For each year of projection, the IBM involves six steps (Fig. 1):

1. Survival of each tree is simulated from a binomial distribution with probability taken from the fitted survival function at the appropriate size.
2. Survivors grow according to the distribution corresponding to their light environment and species identity. The light environment for each individual is determined by its competition index, calculated before starting the IBM and again at the end of each year (step 5).
3. The BA of each individual above the reproductive size threshold is multiplied by the species-specific fecundity parameter (describing the number of recruits per unit BA) corresponding to its light environment to give a per capita contribution to recruitment. Summing across all reproductive individuals gives the total number of recruits per species.
4. Recruits are distributed according to the BA of reproductive adults in each subplot, representing seed dispersal. We enforce density dependence by limiting the number of recruits that enter the plot each year to 0.05 times the starting plot population. Recruits have a higher probability of removal in the density dependence step if located in subplots with high recruit density, representing thinning at the seedling stage, and/or high total BA, representing the increased likelihood of survival in gaps.

5. Competition is recalculated to take into account the growth of existing trees and the addition of new recruits (see below).
6. Return to step 1.

Competition. In the IBM, we allow competition to determine the light environment of every tree. Since height scales with d.b.h., competition is calculated by defining a circle with a 10-m radius around each individual and summing the BA of larger neighbours. We tested the assumption that competition is a good predictor of light, and hence growth, with a linear model of increment growth against competition for each species. There was a statistically significant negative relationship between competition and increment growth for all six species (Table S2).

We use the 5th percentile of competition indices from the 2010 census as the fixed threshold for high light in all years of the IBM; all individuals with competitive indices below this value are assumed to be in high light, while those with competitive indices above this value are assumed to be in low light. In this way, an increase in the number of gaps in the plot results in a higher proportion of individuals included in the high-light environment due to competition indices below the fixed threshold.

EXPERIMENTAL DESIGN AND ANALYSIS

Simulating ash dieback

At the time of writing, ash dieback had not yet arrived in Wytham Woods, thus its effects on mortality at this location was still unknown. To test hypotheses H1 and H4, we explored four possible mortality scenarios with the IBM. In each scenario, we killed *F. excelsior* at a constant rate for the first 10 years of the simulation to bring its population down to either 0%, 25%, 50% or 75% of the initial population size. After 10 years, pathogen-driven mortality was no longer included in the simulations, to allow for the possibility of survival and regeneration of resistant *F. excelsior* individuals. As a baseline, we included a scenario with no ash dieback. For each scenario, we ran 10 stochastic replicated projections for 100 years each. *Fraxinus excelsior* stems were randomly removed each year irrespective of size. We tested a wide range of mortality scenarios to reflect the substantial variation in estimated mortality rates across Europe (e.g. Vasaitis & Lygis 2008; Kirisits & Freinschlag 2012). While some of these scenarios are at the high-end of mortality predictions, they are useful to illustrate more generally the potential impacts of host-specific pests and pathogens and also reflect an observed 'worst case scenario' for *F. excelsior*.

Spatial location

To test whether spatial structure determines regeneration patterns (H3), and allow better extrapolation of results to other forests without the pattern of species distributions observed in our plot, we mixed the locations of stems by sampling without replacement from the observed paired coordinates (Fig. 2b). This enabled us to break down associations between *F. excelsior* and other species while still preserving species' size distributions. We implemented two spatial tests. In one test, *F. excelsior* was included in the spatial randomization, and in the second it was excluded. This changed whether there were many widespread smaller gaps versus fewer large gaps left from the removal of clusters of *F. excelsior*. Gaps of different sizes have been shown to favour recruitment by different species (Kneeshaw & Bergeron 1998), and the different tests were, therefore, expected to lead to different successional outcomes.

Abundance

To test the effect of pre-dieback abundance on the ability of species to colonize the gaps left by *F. excelsior* (H2), we ran the IBM while changing the initial population size of *A. pseudoplatanus* and 'rare canopy' species (Fig. 2c). These projections were compared to the IBMs with observed starting abundances, and differences in population dynamics were interpreted as the effect of initial population sizes. We kept the starting abundance of *F. excelsior* constant so as not to change the amount of gaps produced. The total number of individuals of canopy species remained the same; only the proportions of each species changed, enabling us to maintain a realistic size and spatial structure in the plot while also changing the starting population sizes.

Our main interest was in the effect of starting abundance on the non-native *A. pseudoplatanus* (sycamore), since it is the most abundant species in the 18 ha plot. The different treatments were, therefore, as follows:

1. *Acer pseudoplatanus* and 'rare canopy' started with equal abundance. Other species started at their observed abundances.
2. *Acer pseudoplatanus* started at 10% and 'rare canopy' at 90% of canopy species (excluding *F. excelsior*). Other species started at their observed abundances.
3. *Acer pseudoplatanus* started at 0% and 'rare canopy' at 100% of canopy species (excluding *F. excelsior*). Other species started at their observed abundances.

We tested both the spatial and abundance hypotheses at 75% *F. excelsior* mortality and ran 10 simulations of each treatment for 100 years. We chose this mortality level as it is similar to observed mortality rates in parts of Europe where ash dieback has been established for several decades (Vasaitis & Lygis 2008). It is also high enough to result in many new gaps being formed and thus allowed us to more easily explore the effects of succession.

Demography

The effect of demography was implicitly tested in the hypotheses tests above. After accounting for initial abundances and spatial structure, we were able to determine how much community structure was influenced by differences in demographic strategies. If species were able to invade despite low starting abundances, this was due to highly competitive life history strategies, that is high fecundity, growth rates and/or survival. On the other hand, if a species increased in the standard mortality simulations significantly more than in a simulation in which spatial associations had been broken down, we could conclude that a spatial association with *F. excelsior*, and therefore proximity to gaps left by ash dieback, was partially responsible for its success following *F. excelsior* mortality.

Sensitivity analysis

Fecundity parameters for use in the IBM were inferred from the inverse model based on the assumption that the population growth rate of each species was stable during the census interval ($\lambda = 1$), which is unlikely to have been the case. To test the sensitivity of our results to this assumption, we ran the IBM with either altered fecundity parameters (0.5 or 1.5 times the values inferred from the inverse model) or with fecundity parameters from the inverse model (those that give $\lambda = 1$), but varying levels of density dependence (the num-

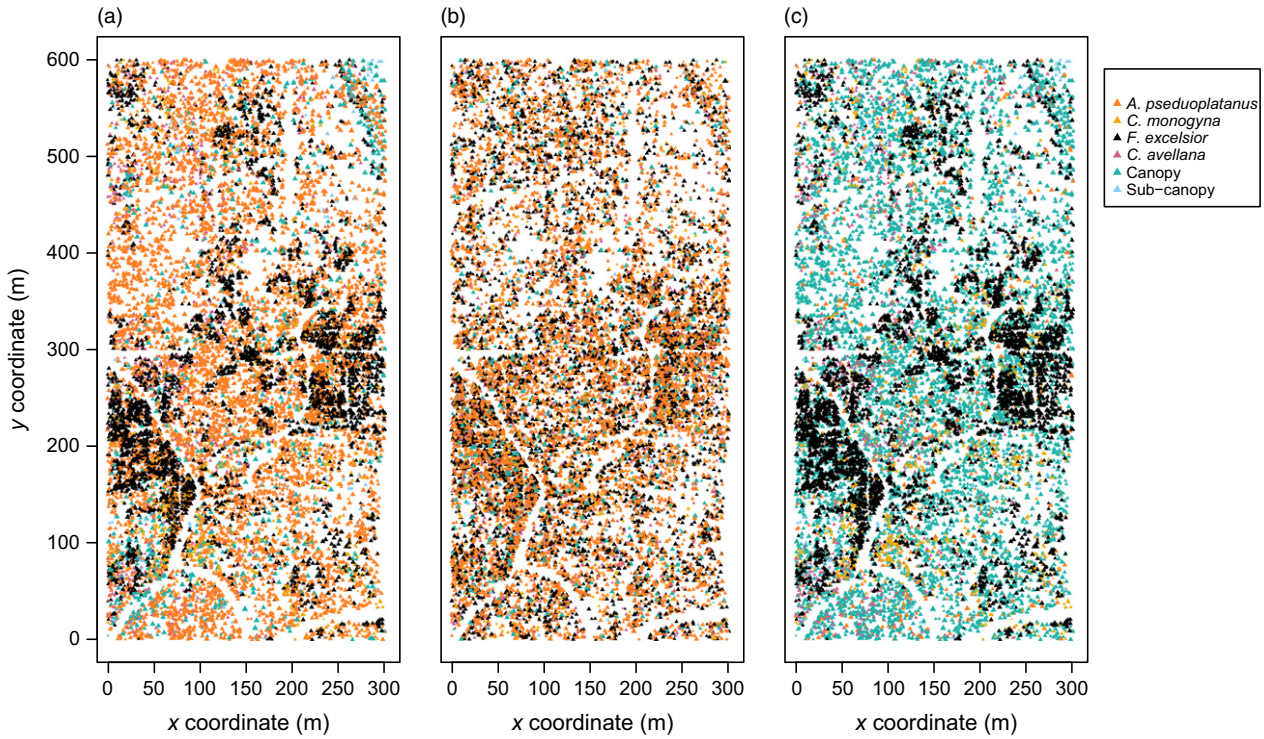

Fig. 2. Maps showing the distribution of individuals at the start of example hypothesis tests, (a) mortality scenarios, (b) spatial randomisation including *Fraxinus excelsior* in the mixing and (c) abundance test with low *Acer pseudoplatanus* starting population. In (c), the ratio of *A. pseudoplatanus* to rare canopy species was changed to 1:9 to test the invasion potential of *A. pseudoplatanus*. Spatial and abundance tests were run at 75% *F. excelsior* mortality. Points are scaled by diameter at breast height.

ber of new recruits each year limited to 0.01 or 0.1 times the starting total plot population). These tests were again run with ash dieback mortality at 75%, similar to mortality rates observed in Europe so far (Vasaitis & Lygis 2008) and high enough to allow easy interpretation of the effect of fecundity parameters and the strength of density dependence in determining the response to the loss of *F. excelsior*.

All work was carried out in R 3.1.2 (R Core Team, 2014), using the MATRIX (Bates & Maechler 2015), SPATIALTOOLS (French 2014) and IGRAPH (Csárdi & Nepusz 2006) packages.

Results

MORTALITY SCENARIOS

The plot's population size and BA were recovered from the loss of a dominant species within 100 years (Figs 3 and 4). In all mortality scenarios, the total BA and population size of the plot initially decreased as the *F. excelsior* population was reduced but remaining canopy species responded to the loss of *F. excelsior* with rapid increases in population size, and after a short lag, increases in BA, such that within a century the total plot BA and population size were above pre-disturbance levels, even in the 100% mortality scenario (see also Tables S6–S10 and S16–S20). 'Rare canopy' species showed the greatest increase in population size in all mortality scenarios, from 856 to 7144 after 100 years in the 75% mortality scenario, but *A. pseudoplatanus* showed the greatest response to the loss of *F. excelsior*, that is a greater increase relative to its trajectory in the no-dieback scenario (Fig. 4). For example, after 100 years, the *A. pseudoplatanus* population had 2124 more individuals in the 75% mortality scenario than in the no-dieback scenario, while the 'rare canopy' population had 1134 more individuals in the 75% mortality scenario compared with the no-dieback scenario. After 100 years, the total plot population size in all mortality scenarios had reached the levels predicted in the no-dieback control. However, due to the large increase in BA of *F. excelsior* in the no-dieback control, total BA m^2 ha^{-1} was still lower in each mortality scenario than in the no-dieback control.

SPATIAL TESTS

The spatial tests had little effect on the plot dynamics (Fig. 5). The *F. excelsior* population recovered marginally better from 75% mortality when there was no mixing of any species compared with either spatial test. 'Rare canopy' species also performed better when spatial distributions were as observed, with a population of 7144 after 100 years in the 75% mortality scenario compared with 6856 and 6780 in the spatial tests including and excluding *F. excelsior,* respectively (Tables S9, S11 and S12). In contrast, *A. pseudoplatanus* had the highest recruitment in the spatial test excluding *F. excelsior* from the mixing. After 100 years, its population was 9358 when all species bar *F. excelsior* were shuffled, compared with 9273 when *F. excelsior* was included in the mixing and 9224 when spatial structure was left as observed in the census. Differences in BA between the two spatial tests

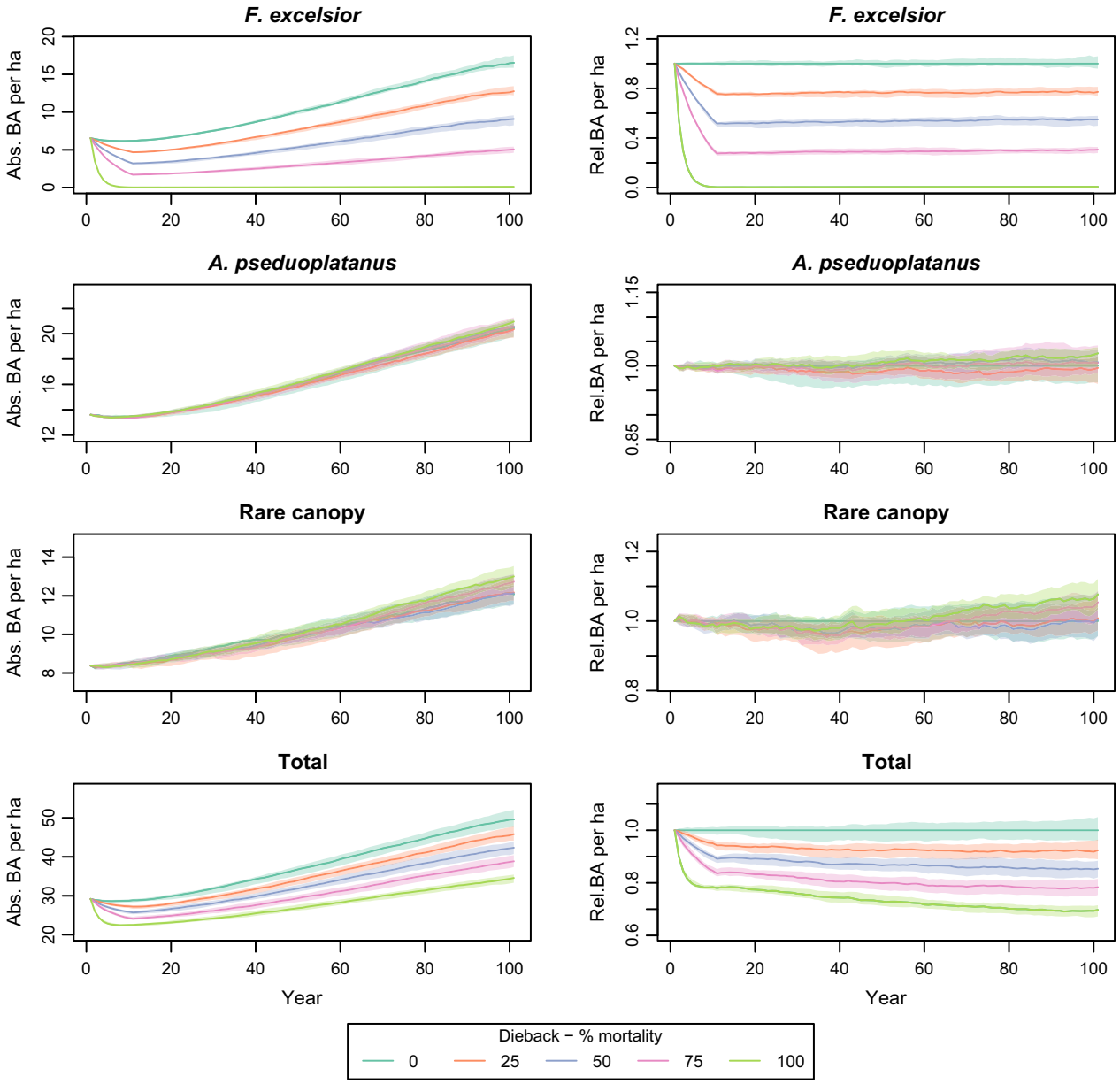

Fig. 3. Basal area (BA m^2 ha^{-1}) of the canopy species and the total BA m^2 ha^{-1} through time, under each mortality scenario. Left-hand panels show absolute BA m^2 ha^{-1}, while right-hand panels show BA m^2 ha^{-1} relative to the 0% mortality scenario (i.e. mortality scenario/0% mortality). Shading depicts 5th and 95th percentiles from 10 simulations at each mortality level. Medians are shown by the darker lines. Both *Acer pseudoplatanus* and rare canopy species increased in BA m^2 ha^{-1} throughout all simulations but increases were greatest in higher dieback scenarios. The BA of *Fraxinus excelsior* recovered well and after 100 years was nearly at pre-disturbance levels even in the 75% mortality scenario.

and the comparison 75% mortality scenario were small for every species (Tables S19, S21, S22).

ABUNDANCE TESTS

When the starting population size of *A. pseudoplatanus* was decreased and made equal to 'rare canopy' species, it was still able to increase rapidly. After approximately 25 years, the population followed the same trajectory as in the 75% mortality scenario, where starting abundances were not manipulated (Fig. 6; Tables S11, S13, S14, S15, S21, S23, S24 and S25). However, when the ratio of *A. pseudoplatanus* stems to 'rare canopy' stems was 1:9, *A. pseudoplatanus* failed to increase to the same extent. After 100 years, the BA of *A. pseudoplatanus* was 3.19 m^2 ha^{-1} when it started rare, compared with 15.29 m^2 ha^{-1} when it started at the same abundance as 'rare canopy' species. 'Rare canopy' species showed a much greater increase in population size and BA when *A. pseudoplatanus* was rare. The total forest population size was also higher in the treatments with *A. pseudoplatanus* low or absent, a result of the increased fecundity of 'rare canopy' species relative to *A. pseudoplatanus*.

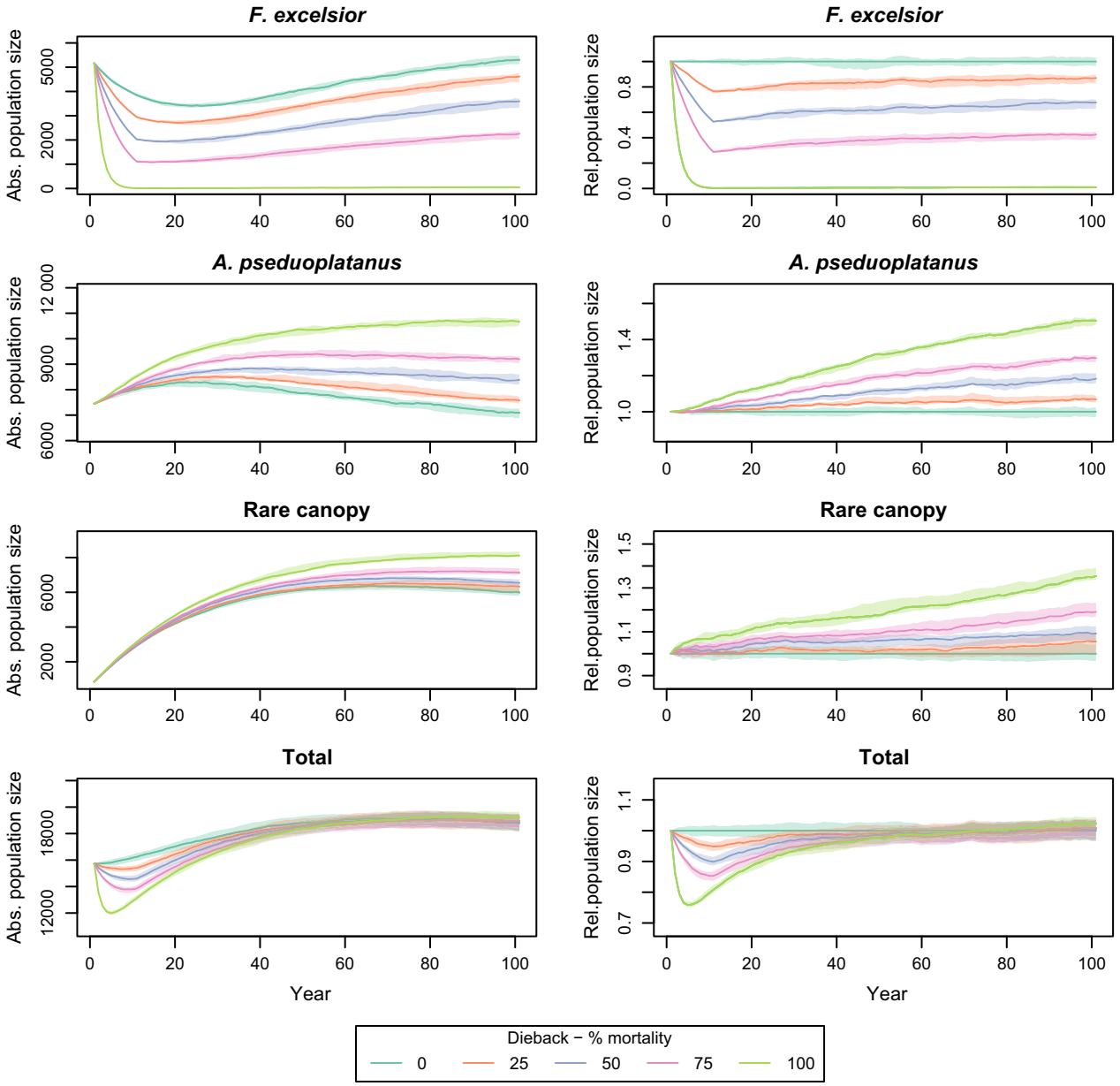

Fig. 4. Population size of canopy species through time, under each mortality scenario. Left-hand panels show absolute population size while right hand panels show population size relative to the 0% mortality scenario (i.e. scenario/0% mortality). Shading depicts the 5th and 95th percentiles from 10 simulations of each scenario. Medians are shown by darker lines. Rare canopy species showed the greatest overall increase in population size whereas *Acer pseudoplatanus* showed the greatest increase in recruitment in response to increasing *Fraxinus excelsior* mortality. The *F. excelsior* population was able to persist in all but the 100% mortality scenario, although it took 100 years for the population to reach pre-disturbance level in the 25% mortality scenario.

SENSITIVITY ANALYSIS

Results from the sensitivity analysis show that density dependence had more effect on the IBM results than fecundity parameters (Figs S14 and S15). The fecundity parameters were inferred in our inverse model based on the assumption of a starting population at equilibrium, that is with a population growth rate ($\lambda = 1$). In our sensitivity analysis, we ran the IBM with fecundity parameters from the inverse model either increased or decreased by 50%. We also ran IBMs in which we changed the strength of density dependence by limiting the number of recruits that enter the plot each year to either 0.01 or 0.1 times the starting total plot population. Changing the strength of density dependence had a much greater effect on the dynamics of the majority of species than altering the fecundity parameters. Qualitatively, the results from the IBMs with altered fecundity parameters were very similar to the IBMs in which we used parameters inferred from inverse model. The sensitivity analysis, therefore, suggests that our IBM results are robust to the necessary inverse model assumption of starting populations at equilibrium.

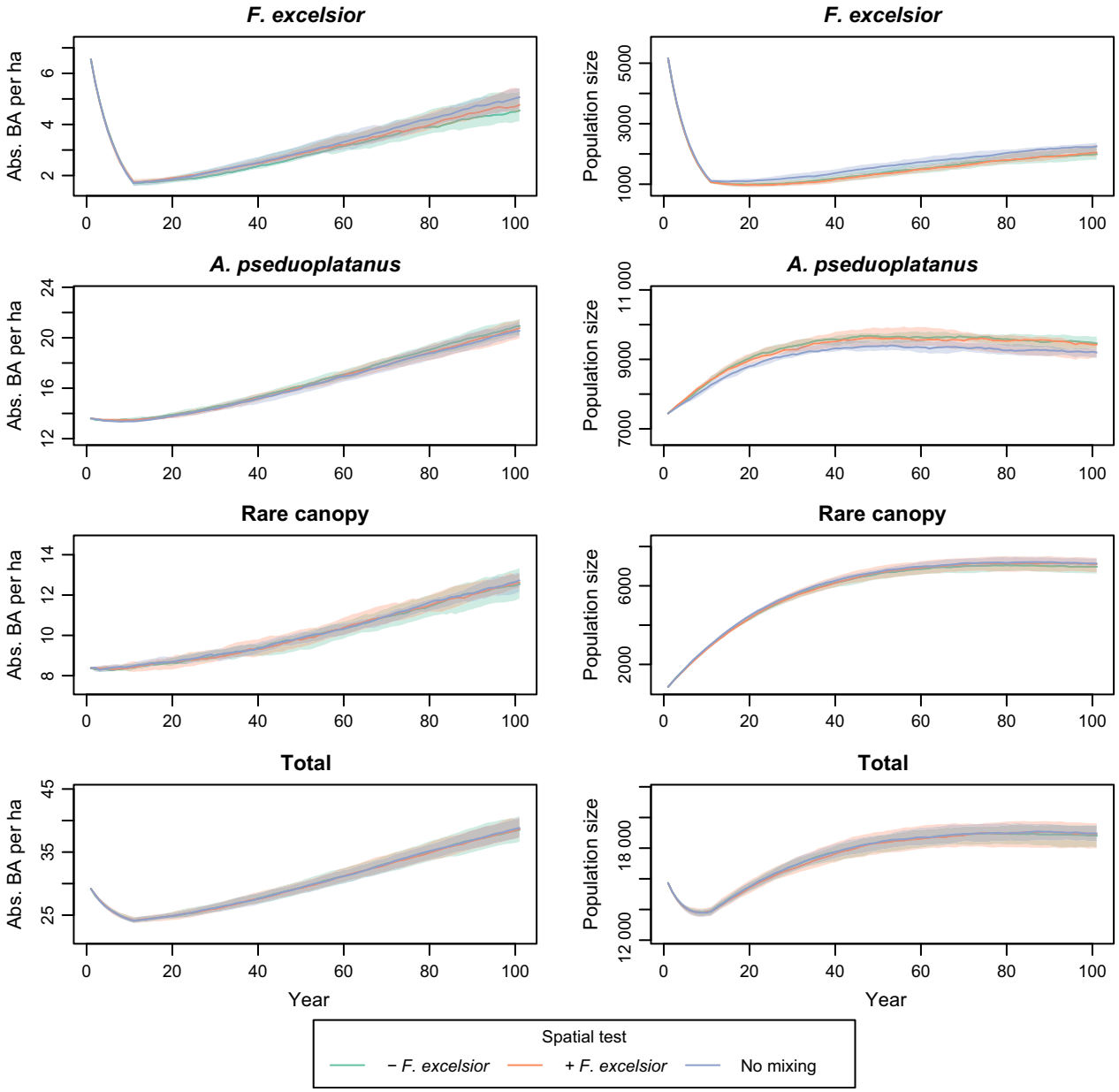

Fig. 5. Results of the spatial randomisation tests showing basal area (BA) m^2 ha^{-1} (left-hand panels) and population size (right-hand panels) of canopy species through time. Spatial randomisation involved reassigning paired coordinates to each stem, with *Fraxinus excelsior* either included (+ *F. excelsior*) or excluded (− *F. excelsior*) from the mixing. Shading depicts the 5th and 95th percentiles from 10 simulations of each scenario. Medians are shown by darker lines. The spatial tests were run at 75% *F. excelsior* mortality which is also plotted for comparison (no mixing). Overall, spatial tests had very little effect on forest dynamics, although *Acer pseudoplatanus* increased more in randomisation tests than in the no mixing scenario, while the opposite was true for *F. excelsior*.

Discussion

Host-specific pathogens that target a dominant forest tree species can cause significant changes to community dynamics including shifts in the size distribution of the host (Peterken & Mountford 1998), changes in the relative abundance of remaining species (Fajvan & Wood 1996) and altered forest biomass (Kurz *et al.* 2008). In our study of the community response to ash dieback in a British woodland, we found that the level of mortality in the host, *F. excelsior* (European ash), determined the extent to which the *F. excelsior* population recovered and the extent of recruitment in remaining species. Further, we found that the starting abundance of each species was an important factor influencing succession. In contrast, spatial associations at this scale (18 ha) had very little impact on the dynamics of remaining species. Our simulations suggest that the *F. excelsior* population could be resilient to mortality even up to 75%. Results indicate that the response of sub-canopy species to the loss of *F. excelsior* will be limited but that *A. pseudoplatanus* and other canopy species will increase in population size, and to a lesser extent BA, as a result of *F. excelsior* decline.

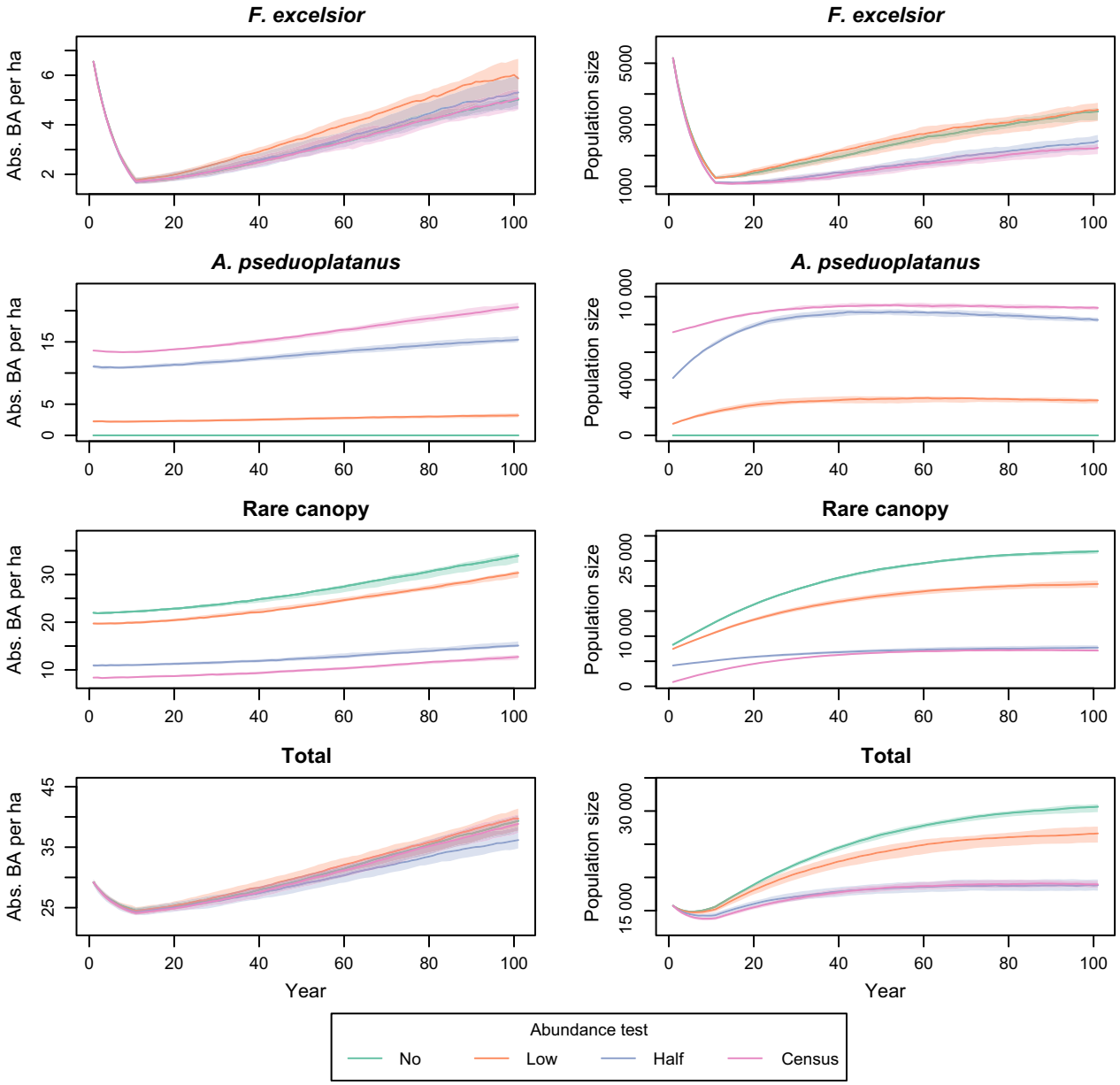

Fig. 6. Results of the abundance tests showing basal area (BA m^2 ha^{-1}) (left-hand panel) and population size (right-hand panel) of canopy species through time. The coordinates of stems remained unchanged from the census data in order to maintain the size and spatial distribution of the forest but the species identity of *Acer pseudoplatanus* and rare canopy species were mixed in various proportions to test the invasion potential of *A. pseudoplatanus*, no (0:1), low (1:9) or half (1:1). The abundance tests were run at 75% *Fraxinus excelsior* mortality, which is also plotted for comparison (census). Shading depicts the 5th and 95th percentiles from 10 simulations of each scenario. Medians are shown by darker lines. The population of *A. pseudoplatanus* increases rapidly in the 1:1 treatment and follows the expected trajectory of the census population, although the regeneration cannot make up the BA in 100 years. In contrast, the population remains much smaller when it starts out low.

FRAXINUS EXCELSIOR DYNAMICS

We found that the long-term *F. excelsior* population dynamics in our plot were extremely sensitive to short-term pathogen-induced mortality. We tested several mortality scenarios with the IBM, killing different percentages of the *F. excelsior* population in the first decade and then allowing the population to recover. We predicted that the *F. excelsior* population would recover from low but not severe mortality scenarios, and that this would impact on the dynamics of remaining species (H1). As expected the *F. excelsior* population showed greater recovery from the lower mortality scenarios. After 100 years, the population size had recovered to near pre-disturbance level in the lowest mortality scenario. However, contrary to predictions, the *F. excelsior* population showed substantial increases, even from a population reduction of 75%. Our results suggest that provided there is a high enough proportion of individuals that are resistant or escape infection, the UK *F. excelsior* population will be able to recover from even high rates of mortality, although recovery to pre-disturbance abundance may take over 100 years. Our results are

contrary to observations from natural forests that have experienced high *F. excelsior* mortality (Lygis *et al.* 2014). However, it is worth noting that in those sites, *F. excelsior* was clear-felled and had resistant adults remained; the level of regeneration may have differed.

The dynamics of the host species following pest or pathogen disturbance depends on a number of factors, such as the level of resistance in the population (King & Lively 2012; Ennos 2015), the number and size distribution of remaining individuals and reservoir hosts (Cobb *et al.* 2012) and the evolution and dynamics of the pathogen (Brasier & Buck 2001). The beetle vector of the Dutch elm disease pathogen preferentially targets larger individuals (Seconca & Leisse 1984), which in places has resulted in the differentiation of *Ulmus* spp. into large sub-populations of small individuals with high regeneration and high mortality and small, isolated sub-populations of larger individuals (Peterken & Mountford 1998). The ash dieback situation is somewhat different, with potentially high mortality across all size classes (Vasaitis & Lygis 2008) but symptoms developing faster in smaller individuals (Keßler *et al.* 2012). The dynamics of the *F. excelsior* population in British woodlands will largely depend on the level of host resistance which is still largely unknown (but see http://oadb.tsl.ac.uk for ongoing research into the genomics of ash dieback resistance), and the evolution of the *H. fraxineus* pathogen. In this study, we assumed that individuals remaining after 10 years of ash dieback either avoided infection or were resistant and produced resistant offspring. Under these circumstances, our results suggest that recovery of *F. excelsior* will be high. However, it is worth noting that if the pathogen persists in the environment and continues to target non-resistant individuals, or evolves to overcome genetic resistance in *F. excelsior*, then eventual mortality rates might be much higher. Although we test a range of mortality scenarios, pathogen dynamics can be complex and unpredictable (Brasier & Buck 2001), and we, therefore, do not attempt to model all possible outcomes.

DYNAMICS OF REMAINING SPECIES

Epidemics in dominant forest species are normally accompanied by changes in community composition. Fajvan & Wood (1996) report that the death of mature canopy oak trees following defoliation by *Lymantria dispar* (gypsy moth) resulted in increases in subdominant *Acer rubrum* (red maples) and *Acer saccharum* (sugar maples). Likewise, since the late 1980s, high mortality due to Dutch elm disease in a temperate Swedish forest has led to increases in species such as *F. excelsior* and *F. sylvatica* (Brunet *et al.* 2014). The main 'winners' in our study were *A. pseudoplatanus* and the 'rare canopy' species, both of which increased in population size and BA, especially when *F. excelsior* mortality was high. In contrast, the sub-canopy species showed little response to *F. excelsior* mortality. These results are consistent with general expectations given the life history strategies of canopy and sub-canopy species. In order to eventually reach the canopy, seedlings and saplings of canopy species must be capable of rapid growth when they find themselves in gaps and access to high light (Canham 1988). In contrast, sub-canopy species are adapted to the lower light levels of the understorey, and while they might respond to an opening of the canopy, it will not be to the same extent as canopy species. In support of this, the parameters for the fast growth distribution that were inferred from the census data were generally lower for the sub-canopy species. It is worth noting that due to our method of pooling rare species, the increases seen by 'rare canopy' can be attributed to increases in ten different species. For example, we did not have the data to model *F. sylavtica* at the species-level, but it could play the role of *A. pseudoplatanus* in other areas of Wytham where *A. pseudoplatanus* is less abundant.

Despite shifts in community composition, European forests generally show high resilience to the decline of a dominant species. For example, in the West-Carpathian fir-beech forests, a 50% decline in the population size and BA of the *Abies alba* (fir) population was accompanied by increased recruitment and growth of remaining species, such that total BA and population size of observed forest stands stabilized within a few decades (Vrška *et al.* 2009). Similar ecosystem resilience was observed following the dieback of *Q. robur* (pedunculate oak) in Central European alluvial hardwood forests (Janík *et al.* 2008).

As expected, remaining canopy species in our simulations showed increases in BA and population size in response to the loss of *F. excelsior* (H1), and after 100 years, the total plot BA and population size were actually higher than the pre-dieback levels (H4). However, *F. excelsior* is known to have high growth rates (Fraxigen, 2005) and was predicted to increase rapidly in BA in our no-dieback simulation. Although in the different mortality scenarios, remaining species filled the gaps left by *F. excelsior* with new recruits, the BA of these small stems could not match the predicted rapid growth of larger *F. excelsior* stems in the no-dieback scenario. These results suggest that the structure of the plot will change in response to ash dieback. In the short-term, an opening of the canopy will lead to the understorey becoming denser due to the increased number of recruits. Overtime, gaps in the canopy will be filled by the growth of existing individuals and the new recruits, such that the BA of the plot recovers to pre-disturbance levels. However, the size structure of the forest will remain more highly skewed towards smaller individuals than it might otherwise have been in a disturbance-free forest.

THE ROLE OF SPATIAL STRUCTURE, STARTING ABUNDANCES AND DEMOGRAPHIC RATES IN DETERMINING SUCCESSION

We predicted that demographic strategy would be more important than starting abundance in determining which species responded most to the loss of *F. excelsior*, and that consequently, *A. pseudoplatanus* would dominate succession even with a reduced starting population (H2). Results supported our hypothesis to an extent, but also showed that with

a very low initial starting population *A. pseudoplatanus* recruitment was limited and the population was unable to dominate the plot.

Results provided little support for H3 that spatial associations between species would determine patterns of succession. We broke down spatial associations between species by reassigning locations to stems, either including or excluding *F. excelsior* in the mixing. Contrary to predictions, the different size and distribution of gaps that this created had little effect on the plot dynamics, with results being very similar between two tests and the comparison mortality scenario. While both *F. excelsior* and 'rare canopy' species showed slightly reduced population increases in the spatial tests, *A. pseudoplatanus* appeared to benefit from the spatial randomization, but only when *F. excelsior* was excluded from spatial mixing. *Fraxinus excelsior* has a clustered distribution in our study plot meaning that high mortality results in gaps that are larger than those normally associated with the loss of a single canopy individual. In plots where *F. excelsior* shows a less clustered distribution gaps will be smaller and more spatially distributed. Our simulation results suggest that *A. pseudoplatanus* will be less successful in such cases. However, with the effect being so small, the spatial tests overall suggest that in this plot, demographic rates influence short mid-term dynamics more than the spatial distribution of species.

ADDITIONAL CONSIDERATIONS

The time frame of transient dynamics in these simulations are important to keep in mind because we know that other factors such as drought and wind-damage influence forest dynamics (Peterken & Jones 1987), and the longer the period before simulated stabilization, the more likely these other stochastic factors will be to alter the course of the forest. For example, an important consideration that may influence the outcome of succession is the drought sensitivity of *A. pseudoplatanus*. Climate projections from Murphy *et al.* (2009) indicate the climate in the south east of England is likely to become hotter and drier with decreased rainfall in the summer months. *Acer pseudoplatanus* has been shown to be particularly sensitive to water stress (Lemoine, Peltier & Marigo 2001; Tissier *et al.* 2004), including at Wytham (Morecroft et al, 2008), and this may limit its ability to dominate over the long-term, despite its success in the transient dynamics forecast here. More generally, models of forest response to pest and pathogen disturbance in areas undergoing rapid climate change or land use change should account for the possibility of much greater impacts due to the increased susceptibility of hosts and the reduced resilience of the whole community (Reyer *et al.* 2015).

Another important consideration is the alternation of regeneration by *F. excelsior* and *A. pseudoplatanus.* In a study of six British woodlands, Waters & Savill (1992) observed that both *F. excelsior* and *A. pseudoplatanus* showed higher recruitment under the canopy of the other species than under a canopy of adults of the same species. A possible consequence of alternation of regeneration is the loss of *F. excelsior* in the canopy limiting regeneration of *A. pseudoplatanus*. However, the study of Waters & Savill (1992) specifically selected sites where reproductive adults of both *A. pseudoplatanus* and *F. excelsior* could contribute seeds to the study plots. Thus, under the *A. pseudoplatanus* canopy, the main competitors to *A. pseudoplatanus* seedlings were *F. excelsior* seedlings. In our study plot, there are areas where *A. pseudoplatanus* is abundant despite *F. excelsior* being nearly absent. This suggests that without competition from *F. excelsior* seedlings, *A. pseudoplatanus* can still have high recruitment under its own canopy. In line with this, our results showed increases in *A. pseudoplatanus* recruitment in response to *F. excelsior* mortality. Morecroft *et al*. (2008) showed that *A. pseudoplatanus* has colonised areas of Wytham where the canopy has been opened up through historical management but has not colonised areas where the canopy has remained closed. This is consistent with our results. It is possible that in the much longer term *A. pseudoplatanus* would decline under closed canopy conditions, especially if this were exacerbated by drought sensitivity.

MODELLING ADVANCES

To predict the dynamics of complex forest communities, ecologists must rely on mechanistic models that combine available data to make scenario-based predictions. Our predictive framework combines these tools to forecast host-specific disease disturbance. The problem of trying to project a whole community forward, based on parameters inferred from just 2 years' worth of data, required an inverse modelling approach to overcome limitations of the short time series available. An example from our analyses highlights an insight that was only possible with the available data by virtue of inverse modelling. We initially used an inverse model that matched the stable size structure from the IPM megamatrix (the normalized dominant right eigenvector) to the observed size distributions from the census data. However, it is clear that due to grazing pressure from fluctuating populations of deer (Perrins & Overall 2001), few of the tree populations in Wytham have a stable size structure. The number of fallow deer (*Dama dama*) and muntjac (*Muntiacus reevesi*) has increased markedly since the 1970s (Perrins & Overall 2001), and the observed tree size distributions have a paucity of smaller size classes (due to grazing) that simply cannot reflect asymptotic dynamics (Fig. S1). Instead, we maximized the likelihood of vital rates models to give a $\lambda = 1$. Although this also assumes that the long-term population growth rate is stable, with an associated stable size structure, it allows the stable size structure to depart from the observed size distribution. Loosening the constraints of the inverse model in this way meant that fecundity parameters producing small individuals did not have a low likelihood in the MCMC analysis, and the resulting parameters are more biologically plausible. In other systems, where population structure is not so heavily influenced by external forces, such as severe herbivory, the use of the stable size distribution from the IPM megamatrix in the inverse modelling framework could further decrease uncertainty in inference of vital rates parameters.

While there is a rapidly growing repository of global forest inventory data, sites with data over long time series are rare. The ability to make inferences about future forest dynamics based upon short time series data is, therefore, critical to enable informed forest management decisions to be made in the majority of areas where long time series of data are unavailable and field experiments are impractical. We have developed a method that makes such inferences possible and allows evaluation of the assumptions needed to connect imperfect data to forecasts. Competitive interactions between individuals are important processes shaping population and community scale patterns. The use of data from a large contiguous plot allowed us to infer these competitive interactions and include them in our simulations of forest dynamics. Our forecasting platform can be readily extended to incorporate other data types such as remote sensing, via inverse modelling, and can explore a wide range of scenario-based forecasts that include different management scenarios.

Conclusions

Wytham Woods is typical of many woodlands in the south of England in terms of its species composition and turnover during the last few decades. As in many forests, *F. excelsior* has increased in abundance while the population of *Q. robur*, English oak, has aged with limited recruitment (Kirby *et al.* 2014). Changes in Wytham following ash dieback are, therefore, likely to reflect changes occurring on a much larger scale. One of the likely successors of *F. excelsior* in Wytham, and many other woodlands across the UK, is *A. pseudoplatanus,* although local patterns of species abundances, size distributions and demographic strategies will influence regeneration in response to ash dieback.

In summary, our modelling results show that forest recovery following epidemics of host-specific pests and pathogens depends on a myriad of factors, but is likely to be dominated by the importance of different demographic strategies which may allow some species to capitalize on a sudden increase in resources.

Acknowledgements

The 18-ha Long-Term Forest Monitoring Plot is a collaborative project between the University of Oxford, the Centre for Ecology and Hydrology, and the Smithsonian Institution CTFS Forest-GEO (HSBC Climate Partnership). Thanks go to Prof. Hal Caswell for assistance with the megamatrix construction. Much of the early work on this project was carried out at a CTFS Forest-GEO meeting for which JN received a travel grant from the Department of Plant Sciences, Oxford. SMM and CM were partially funded by the USA National Science Foundation (NSF 640261 to SMM). This work forms part of JN's DPhil which is funded by a Clarendon Scholarship, a New College Scholarship and the BBSRC. JN would like to give special thanks to Dr. Roosa Leimu-Brown, Dr. Charlotte Metcalf and Dr. Nick Brown for their valuable supervisory support throughout her DPhil. The authors declare no conflict of interests.

Data accessibility

The data are archived in the Smithsonian Institution's Forest Global Earth Observatory site and can be accessed by request from: http://ctfs.si.edu/Public/plotdataaccess/index.php. See Butt *et al.* (2010).

References

Bates, D. & Maechler, M. (2015) *Matrix: Sparse and Dense Matrix Classes and Methods*. R package version 1.1-5. http://CRAN.R-project.org/package=-Matrix.

Beaumont, M.A. (2010) Approximate Bayesian computation in evolution and ecology. *Annual Review of Ecology, Evolution and Systematics*, **41**, 379–406.

Besbeas, P., Lebreton, J.-D. & Morgan, B.J.T. (2003) The efficient integration of abundance and demographic data. *Journal of the Royal Statistical Society: Series C (Applied Statistics)*, **52**, 95–102.

Brasier, C.M. (2008) The biosecurity threat to the UK and global environment from international trade in plants. *Plant Pathology*, **57**, 792–808.

Brasier, C.M. & Buck, K.W. (2001) Rapid evolutionary changes in a globally invading fungal pathogen (Dutch elm disease). *Biological Invasions*, **3**, 223–233.

Brunet, J., Bukina, Y., Hedwall, P.-O., Holmström, E. & von Oheimb, G. (2014) Pathogen induced disturbance and succession in temperate forests: evidence from a 100-year data set in southern Sweden. *Basic and Applied Ecology*, **15**, 114–121.

Butt, N., Campbell, G., Malhi, Y., Morecroft, M., Fenn, K. & Thomas, M. (2009) Initial results from establishment of a long-term broadleaf monitoring plot at Wytham Woods, Oxford, UK. University of Oxford Report. University of Oxford, Oxford, UK.

Butt, N., Marthews, T., Mahli, Y. & Morecroft, M. (2010) Wytham Woods forest plot data. URL: http://ctfs.si.edu/Public/plotdataaccess/SiteDescription.php?plotname=wytham+woods&typedata=tree

Canham, C. (1988) Growth and canopy architecture of shade-tolerant trees: response to canopy gaps. *Ecology*, **69**, 786–795.

Caswell, H. (2001) *Matrix Population Models: Construction, Analysis and Interpretation*. Sinauer Associates, Sunderland, MA, USA.

Caswell, H. (2012) Matrix models and sensitivity analysis of populations classified by age and stage: a vec-permutation matrix approach. *Theoretical Ecology*, **5**, 403–417.

Clebsch, E.E.C. & Busing, R.T. (1989) Secondary succession, gap dynamics, and community structure in a southern Appalachian cove forest. *Ecology*, **70**, 728–735.

Cobb, R.C., Filipe, J.A.N., Meentemeyer, R.K., Gilligan, C.A. & Rizzo, D.M. (2012) Ecosystem transformation by emerging infectious disease: loss of large tanoak from California forests. *Journal of Ecology*, **100**, 712–722.

Comita, L.S., Aguilar, S., Perez, R., Lao, S. & Hubell, S.P. (2007) Patterns of woody plant species abundance and diversity in the seedling layer of a tropical forest. *Journal of Vegetation Science*, **18**, 163–174.

Condit, R. (1998) *Tropical Forest Census Plots: Methods and Results from Barro Colorado Island, Panama and a Comparison with Other Plots*. Springer-Verlag and R. G. Landes Company, Berlin, Germany.

CRU CL2.0 Climate Research Unit, University of East Anglia, available at http://www.cru.uea.ac.uk

Csárdi, G. & Nepusz, T. (2006) The igraph software package for complex network research. *InterJournal, Complex Systems*, **1695**, 1695–1704.

Easterling, M.R., Ellner, S.P. & Dixon, P.M. (2000) Size-specific sensitivity: applying a new structured population model. *Ecology*, **81**, 694–708.

Ellison, A.M., Bank, M.S., Clinton, B.D., Colburn, E.A., Elliott, K., Ford, C.R. *et al.* (2005) Loss of foundation species: consequences for the structure and dynamics of forested ecosystems. *Frontiers in Ecology and the Environment*, **3**, 479–486.

Ennos, R.A. (2015) Resilience of forests to pathogens: an evolutionary ecology perspective. *Forestry*, **88**, 41–52.

Eschtruth, A.K., Cleavitt, N.L., Battles, J.J., Evans, R.A. & Fahey, T.J. (2006) Vegetation dynamics in declining eastern hemlock stands: 9 years of forest response to hemlock woolly adelgid infestation. *Canadian Journal of Forest Research*, **36**, 1435–1450.

Fajvan, M. & Wood, J.M. (1996) Stand structure and development after gypsy moth defoliation in the Appalachian Plateau. *Forest Ecology and Management*, **89**, 79–88.

FAO. (2010) Global forest resources assessment 2010. Food and Agricultural Organization of the United Nations, Rome, Italy.

Ford, C.R., Elliott, K.J., Clinton, B.D., Kloeppel, B.D. & Vose, J.M. (2012) Forest dynamics following eastern hemlock mortality in the southern Appalachians. *Oikos*, **121**, 523–536.

Fraxigen. (2005) *Ash Species in Europe: Biological Characteristics and Practical Guidelines for Sustainable use*. Oxford Forestry Institute University of Oxford, Oxford, UK.

Frelich, L.E. & Reich, P.B. (1995) Spatial patterns and succession in a Minnesota southern-boreal forest. *Ecological Monographs*, **65**, 325–346.

French, J. (2014) *SpatialTools: Tools for Spatial Data Analysis*. R package version 0.5.8. http://CRAN.R-project.org/package=SpatialTools.

Gelman, A. & Hill, J. (2007) *Data Analysis Using Regression and Multi-Level/Hierarchical Models*. Cambridge University Press, New York, NY, USA.

Gelman, A., Carlin, J.B., Stern, H.S., Dunson, D.B., Vehtari, A. & Rubin, D.B. (2013) *Bayesian Data Analysis*, 3rd edn. Chapman and Hall/CRC, Boca Raton, FL, USA.

González, E.J. & Martorell, C. (2013) Reconstructing shifts in vital rates driven by long-term environmental change: a new demographic method based on readily available data. *Ecology and Evolution*, **3**, 2273–2284.

Gross, A., Holdenrieder, O., Pautasso, M., Queloz, V. & Sieber, T.N. (2014) Hymenoscyphus pseudoalbidus, the causal agent of European ash dieback. *Molecular Plant Pathology*, **15**, 5–21.

Hartig, F., Dislich, C., Wiegand, T. & Huth, A. (2014) Technical note: approximate Bayesian parameterization of a process-based tropical forest model. *Biogeosciences*, **11**, 1261–1272.

Hastings, W.K. (1970) Monte Carlo sampling methods using Markov chains and their applications. *Biometrika*, **57**, 97–109.

Hicke, J.A., Allen, C.D., Desai, A.R., Dietze, M.C., Hall, R.J., Hogg, E.H., Kashian, D.M., Moore, D., Raffa, K.F., Sturrock, R.N. & Vogelmann, J. (2012) Effects of biotic disturbances on forest carbon cycling in the United States and Canada. *Global Change Biology*, **18**, 7–34.

Janík, D., Adam, D., Vrška, T., Hort, L., Unar, P., Horal, D., Král, K. & Šamonil, P. (2008) Tree layer dynamics of the Cahnov-Soutok near natural floodplain forest after 33 years (1973–2006). *European Journal of Forest Research*, **127**, 337–345.

Jönsson, M.T. & Thor, G. (2012) Estimating coextinction risks from epidemic tree death: affiliate lichen communities among diseased host tree populations of *Fraxinus excelsior*. *PLoS One*, **7**, e45701.

Keßler, M., Cech, T.L., Brandstetter, M. & Kirisits, T. (2012) Dieback of ash (*Fraxinus excelsior* and *Fraxinus angustifolia*) in Eastern Austria: disease development on monitoring plots from 2007 to 2010. *Journal of Agricultural Extension and Rural Development*, **4**, 223–226.

King, K.C. & Lively, C.M. (2012) Does genetic diversity limit disease spread in natural host populations? *Heredity*, **109**, 199–203.

Kirby, K.J., Bazely, D.R., Goldberg, E.A., Hall, J.E., Isted, R., Perry, S.C. & Thomas, R.C. (2014) Changes in the tree and shrub layer of Wytham Woods (Southern England) 1974–2012: local and national trends compared. *Forestry*, **87**, 663–673.

Kirisits, T. & Freinschlag, C. (2012) Ash dieback caused by *Hymenoscyphus pseudoalbidus* in a seed plantation of *Fraxinus excelsior* in Austria. *Journal of Agricultural Extension and Rural Development*, **4**, 184–191.

Kjær, E.D., McKinney, L.V., Nielsen, L.R., Hansen, L.N. & Hansen, J.K. (2012) Adaptive potential of ash (*Fraxinus excelsior*) populations against the novel emerging pathogen *Hymenoscyphus pseudoalbidus*. *Evolutionary Applications*, **5**, 219–228.

Kneeshaw, D.D. & Bergeron, Y. (1998) Canopy gap characteristics and tree teplacement in the southeastern Boreal forest. *Ecology*, **79**, 783–794.

Kurz, W.A., Dymond, C.C., Stinson, G., Rampley, G.J., Neilson, E.T., Carroll, A.T., Ebata, T. & Safranyik, L. (2008) Mountain pine beetle and forest carbon feedback to climate change. *Nature*, **452**, 987–990.

Lemoine, D., Peltier, J.P. & Marigo, G. (2001) Comparative studies of the water relations and the hydraulic characteristics in *Fraxinus excelsior*, *Acer pseudoplatanus* and *A. opalus* trees under soil water contrasted conditions. *Annals Forest Science*, **58**, 723–731.

Logan, J.A. & Powell, J.A. (2001) Ghost forest, global warming and the mountain pine beetle (Coleoptera: Scolyttidae). *American Entomologist*, **47**, 160–172.

Loo, J.A. (2009) Ecological impacts of non-indigenous invasive fungi as forest pathogens. *Biological Invasions*, **11**, 81–96.

Lygis, V., Bakys, R., Gustiene, A., Burokiene, D., Matelis, A. & Vasaitis, R. (2014) Forest self-regeneration following clear-felling of dieback-affected *Fraxinus excelsior*: focus on ash. *European Journal of Forest Research*, **133**, 501–510.

McKinney, L.V., Thomsen, I.M., Kjaer, E.D., Bengtsson, S.B.K. & Nielsen, L.R. (2012) Rapid invasion by an aggressive pathogenic fungus (*Hymenoscyphus pseudoalbidus*) replaces a native decomposer (*Hymenoscyphus albidus*): a case of local cryptic extinction? *Fungal Ecology*, **5**, 663–669.

McKinney, L.V., Nielsen, L.R., Collinge, D.B., Thomsen, I.M., Hansen, J.K. & Kjær, E.D. (2014) The ash dieback crisis: genetic variation in resistance can prove a long-term solution. *Plant Pathology*, **63**, 485–499.

Merow, C., Dahlgren, J.P., Metcalf, C.J.E., Childs, D.Z., Evans, M.E.K., Jongejans, E., Record, S., Rees, M., Salguero-Gómez, R. & McMahon, S.M. (2014) Advancing population ecology with integral projection models: a practical guide. *Methods in Ecology and Evolution*, **5**, 99–110.

Metcalf, C.J.E., Horvitz, C.C., Tuljapukar, S. & Clark, D.A. (2009) A time to grow and a time to die: a new way to analyze the dynamics of size, light, age and death of tropical trees. *Ecology*, **90**, 2766–2778.

Mitchell, R.J., Beaton, J.K., Bellamy, P.E., Broome, A., Chetcuti, J., Eaton, S. *et al.* (2014) Ash dieback in the UK: a review of the ecological and conservation implications and potential management options. *Biological Conservation*, **175**, 95–109.

Morecroft, M.D., Stokes, V.J., Taylor, M.E. & Morison, J.I.L. (2008) Effects of climate and management history on the distribution and growth of sycamore (*Acer pseudoplatanus* L.) in a southern British woodland in comparison to native competitors. *Forestry*, **81**, 59–74.

Morris, W.F. & Doak, D.F. (2002) *Quantitative Conservation Biology: Theory and Practice of Population Viability Analysis*. Sinauer Associates Inc., Sunderland, MA, USA.

Murphy, J., Sexton, D., Jenkins, G., Boorman, P., Booth, B., Brown, C. *et al.* (2009) *UK Climate Projections Science Report: Climate Change Projections*. Meteorological Office Hadley Centre, Exeter, UK.

National Forest Inventory, F.C. (2012) NFI preliminary estimates of quantities of broadleaved species in British woodlands, with special focus on ash. Forestry Commission, Edinburgh, UK

Pautasso, M., Aas, G., Queloz, V. & Holdenrieder, O. (2013) European ash (*Fraxinus excelsior*) dieback – a conservation biology challenge. *Biological Conservation*, **158**, 37–49.

Perrins, C.M. & Overall, R. (2001) Effect of increasing numbers of deer on bird populations in Wytham Woods, central England. *Forestry*, **74**, 299–309.

Peterken, G.F. & Jones, E.W. (1987) Forty years of change in lady park wood: the old-growth stands. *Journal of Ecology*, **75**, 477–512.

Peterken, G.F. & Mountford, E.P. (1998) Long-term change in an unmanaged population of wych elm subjected to Dutch elm disease. *Journal of Ecology*, **86**, 205–218.

Pliūra, A., Lygis, V., Suchockas, V. & Bartkevičius, E. (2011) Performance of twenty four European *Fraxinus excelsior* populations in three Lithuanian progeny trials with a special emphasis on resistance to *Chalara fraxinea*. *Baltic Forestry*, **17**, 17–34.

Przybyl, K. (2002) Fungi associated with necrotic apical parts of *Fraxinus excelsior* shoots. *Forest Pathology*, **32**, 387–394.

R Core Team. (2014) *R: A Language and Environment for Statistical Computing*. R Foundation for Statistical Computing, Vienna, Austria.

Reyer, C.P.O., Brouwers, N., Rammig, A., Brook, B.W., Epila, J., Grant, R.F. *et al.* (2015) Forest resilience and tipping points at different spatio-temporal scales: approaches and challenges. *Journal of Ecology*, **103**, 5–15.

Rüger, N. & Condit, R. (2012) Testing metabolic theory with models of tree growth that include light competition. *Functional Ecology*, **26**, 759–765.

Savill, P., Perrins, C., Kirby, K. & Fisher, N. (2010) *Wytham Woods: Oxford's Ecological Laboratory*. Oxford University Press, Oxford, UK.

Seconca, C. & Leisse, N. (1984) Significance of bark beetles Coleoptera Scolytidae in the spread of Dutch elm disease in the area Euskirchen West Germany. *Zeitschrift Angewandte Entomologie*, **98**, 413–423.

Tingley, M.W., Orwig, D.A., Field, R. & Motzkin, G. (2002) Avian response to removal of a forest dominant: consequences of hemlock woolly adelgid infestations. *Journal of Biogeography*, **29**, 1505–1516.

Tissier, J., Lambs, L., Peltier, J.P. & Marigo, G. (2004) Relationships between hydraulic traits and habitat preference for six *Acer* species occurring in the French Alps. *Annals of Forest Science.*, **61**, 81–86.

Vasaitis, R. & Lygis, V. (2008) Emerging Forest Disease in South-eastern Baltic Sea Region. Network of Climate Change Risks on Forests (ForRisk). SNS Workshop, Umea, Sweden, pp. 14–15.

Vrška, T., Adam, D., Hort, L., Kovár, T. & Janík, D. (2009) European beech (*Fagus sylvatica* L.) and silver fir (*Abies alba* Mill.) rotation in the Carpathians – a developmental cycle or a linear trend induced by man? *Forest Ecology and Management*, **258**, 347–356.

Waters, T.L. & Savill, P. (1992) Ash and sycamore regeneration and the phenomenon of their alternation. *Forestry*, **65**, 417–433.

Whitmore, F.C. (1998) *An Introduction to Tropical Rain Forests*. Oxford University Press, Oxford, UK.

Wood, S. N. (1997) Structured population models in marine, terrestrial and freshwater systems. *Inverse Problems and Structured-Population Dynamics* (eds S. Tuljapurkar & H. Caswell), pp. 555–586. Springer, Chapman and Hall, London, UK.

Received 7 June 2015; accepted 20 January 2016
Handling Editor: Alden Griffith

Supporting Information

Additional Supporting Information may be found in the online version of this article:

Figure S1. Density plots showing the size distribution of each species.

Figure S2. Mean monthly temperatures and precipitation for Wytham Woods for the thirty years up to, and including the census interval.

Figure S3. Schematic of the survival function showing the effect of altering each parameter.

Figure S4. Survival probability for each species.

Figure S5. Histogram of the annual growth increment data from the Wytham census data.

Figure S6. Growth distributions for each species.

Figure S7. Fecundity function for each species.

Figure S8. Schematic of the megamatrix that moves individuals between sizes and light environments.

Figure S9. Schematic of the transition probabilities between the light environments, used to construct the megamatrix.

Figure S10. Basal area of the sub-canopy species through time under each mortality scenario.

Figure S11. Population size of sub-canopy species through time under each mortality scenario.

Figure S12. Results of the spatial randomization tests showing basal area and population size of sub-canopy species through time.

Figure S13. Results of the abundance test showing basal area and population size of sub-canopy species through time.

Figure S14. Results of the sensitivity analysis showing the basal area and population size of canopy species through time.

Figure S15. Results of the sensitivity analysis showing the basal area and population size of sub-canopy species through time.

Figure S16. Basal area of the canopy species under each mortality scenario separated by recruits and existing individuals.

Table S1. Population sizes and species groupings.

Table S2. Slopes and statistical significance of the relationship between competition and growth for each species.

Table S3. Survival parameters for each species.

Table S4. Growth parameters for each species.

Table S5. Fecundity parameters for each species.

Table S6. Population size of each species every 25 years in the 0% mortality scenario.

Table S7. Population size of each species every 25 years in the 25% mortality scenario.

Table S8. Population size of each species every 25 years in the 50% mortality scenario.

Table S9. Population size of each species every 25 years in the 75% mortality scenario.

Table S10. Population size of each species every 25 years in the 100% mortality scenario.

Table S11. Population size of each species every 25 years in the spatial randomization test including *F. excelsior* in the mixing.

Table S12. Population size of each species every 25 years in the spatial randomization test excluding *F. excelsior* from the mixing.

Table S13. Population size of each species every 25 years in the abundance test with equal starting population sizes of *A. pseudoplatanus* and 'rare canopy' species.

Table S14. Population size of each species every 25 years in the abundance test with *A. pseudoplatanus* and 'rare canopy' species starting in the ratio 1:9.

Table S15. Population size of each species every 25 years in the abundance test with *A. pseudoplatanus* absent.

Table S16. Basal area of each species every 25 years in the 0% mortality scenario.

Table S17. Basal area of each species every 25 years in the 25% mortality scenario.

Table S18. Basal area of each species every 25 years in the 50% mortality scenario.

Table S19. Basal area of each species every 25 years in the 75% mortality scenario.

Table S20. Basal area of each species every 25 years in the 100% mortality scenario.

Table S21. Basal area of each species every 25 years in the spatial randomization test including *F. excelsior* in the mixing.

Table S22. Basal area of each species every 25 years in the spatial randomization test excluding *F. excelsior* from the mixing.

Table S23. Basal area of each species every 25 years in the abundance test with equal starting population sizes of *A. pseudoplatanus* and 'rare canopy' species.

Table S24. Basal area of each species every 25 years in the abundance test with *A. pseudoplatanus* and 'rare canopy' species starting in the ratio 1:9.

Table S25. Basal area of each species every 25 years in the abundance test with *A. pseudoplatanus* absent.

Table S26. Summary of each effect tested, the *F. excelsior* mortality level and the hypothesis it relates to.